J Therm Anal Calorim (2010) 99:583–592
DOI 10.1007/s10973-009-0609-z

Propyl paraben-induced changes in dipalmitoyl phosphatidylethanolamine vesicles

Lata Panicker

Received: 31 March 2009 / Accepted: 17 November 2009 / Published online: 11 December 2009

Abstract This article reports the influence of the preservative, propyl paraben (PPB), on the phase transition and dynamics of dipalmitoyl phosphatidylethanolamine (DPPE) vesicles both in multilamellar vesicular (MLV) and unilamellar vesicular (ULV) forms using DSC and (^{1}H and ^{31}P) NMR. DSC results indicate that the mechanism by which PPB interacts with DPPE vesicles is similar in both forms. Addition of PPB to DPPE dispersion results in lowering of the gel to liquid crystalline phase transition temperature (T_m) and consequently increases DPPE headgroup fluidity. At high PPB concentration, additional transitions are observed whose intensity increases with increasing PPB concentration. DSC and NMR data indicate that the PPB molecules get intercalated between the DPPE headgroups as the polar group of the PPB molecules interacts with the polar group of PE, and the alkyl chain of PPB penetrates into the acyl chain region. The interesting finding with MLV is that the gel phase of DPPE in the presence of PPB, on equilibration at 25 °C, transforms to a stable crystalline subgel phases and whose intensity increases with increasing PPB concentration. The effect of inclusion of cholesterol in the PPB-free and PPB-doped DPPE dispersion was also studied.

Keywords DPPE · Differential scanning calorimetry · NMR · Propyl paraben

L. Panicker (✉)
Solid State Physics Division, Bhabha Atomic Research Centre, Mumbai 400 085, India
e-mail: Lata_Panicker@yahoo.com; lata@barc.gov.in

Introduction

Propyl paraben (PPB) with pK_a value of 8.47 has both antimicrobial and antioxidant activity [1] and is effective in the pH range of 3–9. It is effective against yeast, molds, and gram-positive bacteria. PPB, because of its antimicrobial activity [2, 3] and relatively low toxicity in humans, is used as preservative in foods, cosmetics, toiletries, and pharmaceuticals. The mechanism by which paraben acts is mainly by causing disorganization of the microbial cell membrane: (a) at low (bacteriostatic) concentrations, parabens appear to cause energy uncoupling which inhibits the uptake of metabolites and (b) at higher (bactericidal) concentrations, loss of the membrane semipermeability occurs [4–7]. Parabens, thus, inhibit the growth of microorganisms. However, in recent years, the toxicity and cancerigoneous potential of parabens have been raised in membrane studies [8, 9].

Hence, it is important to understand at a molecular level the mode of action of PPB with biomembranes and proteins. As a starting step toward understanding PPB-biomembrane interaction, one studies its interactions with the model membranes. Phospholipids, one of the important constituents of biomembranes, are often used to form the model-membrane system. Phosphatidylethanolamine (PE) and phosphatidylcholine (PC) are major phospholipids found in biomembranes [10]. At pH 7.4, both PC and PE are zwitterionic. In this study, a dispersion of dipalmitoyl phosphatidylethanolamine (DPPE) in buffer is used as the model membrane system.

Earlier studies with PPB-doped dipalmitoyl phosphatidic acid (DPPA) and dipalmitoyl phosphatidylcholine (DPPC) dispersions showed that PPB interacts with DPPA and DPPC vesicle by affecting both their thermotropic behavior and molecular mobility [11, 12]. The nature of

interaction in DPPA dispersion was found to depend on the concentration of the preservative used: (a) at low PPB concentration, PPB increases the membrane headgroup fluidity and decreases the acyl chain rigidity and (b) at high PPB concentration, PPB increases both the membrane headgroup fluidity and the acyl chain rigidity. However, with DPPC dispersion, such a concentration dependence was not seen and for the PPB concentration used the membrane headgroup fluidity increases and the acyl chain rigidity decreases. Prolonged equilibration of PPB-doped MLV of DPPA and DPPA-cholesterol resulted in the formation of a stable crystalline phase. This stable crystalline phase seems to be more ordered (as indicated by large enthalpy values) than the gel, L_{β}, phase. Hence PPB converts the gel phase of DPPA to a metastable gel phase which on equilibration transforms to stable crystalline phase. Such behavior was not seen with PPB-doped MLV of DPPC and DPPC-cholesterol. The observed differences seem to be related to (i) the stronger PA–PA headgroup interaction than PC–PC and (ii) the difference in the headgroup charge (DPPA is negatively charged at pH 7.4 while DPPC is zwitterionic at pH 7.4). Time-dependent studies with DPPA and DPPC dispersions (no change in the thermal parameters) suggest that PPB molecules are very strongly bound and remain intercalated between the polar headgroups for prolonged time.

In order to see what type of interactions take place between PPB and DPPE vesicles, studies were carried out with PPB doped DPPE dispersions using DSC and (^{1}H and ^{31}P) NMR.

Materials and methods

Sample preparation

Lipid, L-α-DPPE, was purchased from Avanti Polar Lipids, Inc., Alabama, USA, and was used without further purification. The preservative, PPB (99+% purity), and cholesterol (from porcine liver, >99% purity) were obtained from Aldrich Chemical Company, Inc., USA. The buffer of (i) pH 7.4 was prepared using 10 mM di-sodium hydrogen orthophosphate (Na_2HPO_4) and 10 mM sodium dihydrogen orthophosphate (NaH_2PO_4) solutions; to this buffer 0.9% (w/w) NaCl was added and (ii) pH 9.3 was prepared using 0.2 M boric acid and 0.05 M borax ($Na_2B_4O_7 \cdot 10\ H_2O$) solutions. The model membranes used in this investigation were in multilamellar vesicular (MLV) and unilamellar vesicular (ULV) forms. The method of preparation of the membrane samples in the MLV and ULV forms is detailed elsewhere [13–15]. The mass ratio of DPPE:cholesterol(ch) is 3:1. The mass fraction of buffer to DPPE is 2.5 in MLV. The lipid concentration, [DPPE], in the case of ULV, is 25 mM. The molar ratio, R_m, of PPB to DPPE is in the range, $0 \leq R_m \leq 0.4$. Systematic studies carried out with DPPE dispersions prepared at different pHs show that DPPE forms stable ULV at pH $\geq$ 9.3 when sonicated for 10 min (forms translucent dispersion). However, at pH < 9.3 DPPE does not form stable ULV even under sonication for an hour (the DPPE dispersion continues to remain milky indicating the presence of MLV also). Hence, the ULV of DPPE was prepared using buffer pH 9.3 [14, 15].

For DSC measurements, 7–12 mg (for MLV) and 15–18 mg (for ULV) of the samples were hermetically sealed in aluminum pans. In order to obtain NMR spectra, approximately 1 mL of ULV was taken in a conventional NMR tube. TLC studies on the samples were carried out to check the intactness of the lipid and PPB molecules.

Differential scanning calorimeter

Mettler Toledo DSC 822 was used for thermal measurements of the membrane samples, with an empty aluminum pan as a reference. Temperature and enthalpy calibrations of the instrument were done, using cyclohexane and indium at a heating rate of 10 °C/min. The chain melting (CM) transition temperature, T_m, was obtained by extrapolating the transition peak temperatures (obtained at scanning speed of 10, 5, and 2 °C/min) to zero scanning speed. The transition enthalpy, ΔH_m, of the endothermic curve reported is the average of the enthalpy values obtained from 5 to 2 °C/min scans. The values of full width at half maximum, Δ_m, used to compare the cooperativity of the CM transitions were obtained from 5 °C/min scans. The DSC measurements were carried out both for the MLV and the ULV. Experiments were carried out immediately after the preparation ($\tau_e \approx 0$) of the respective (MLV and ULV) membrane samples. Experiments were repeated again after equilibrating the samples (a) for 1 day ($\tau_e \approx 1$ day) at 25 °C and (b) for 7 days ($\tau_e \approx 7$ days) at 25 °C. For each value of the molar ratio, R_m, the experiment was repeated with at least three samples. Data were considered only for those samples in which mass loss was less than 0.2 mg at the end of the scanning experiments.

Nuclear magnetic resonance

^{1}H and ^{31}P Nuclear magnetic resonance (NMR) spectra were recorded on a Bruker Avance 500 spectrometer equipped with a calibrated temperature control at 500 and 202 MHz, respectively. The instrumental parameters used to carry out the experiments are detailed elsewhere [15]. The conventional 5 mm NMR tube containing approximately 1 mL of ULV solution was used to record both ^{1}H and ^{31}P NMR spectra. D_2O and H_3PO_4 (85%) were used as

external references for ^{1}H and ^{31}P NMR experiments, respectively. The NMR spectra were recorded in the vicinity of the chain melting transition temperatures of the ULV. At each temperature the samples were equilibrated in the NMR spectrometer for at least 10 min before recording the spectra.

Results

DSC—multilamellar vesicles

$\tau_e \approx 0$

The DSC heating scans of DPPE multilamellar vesicles (MLV) in buffer pH 7.4 obtained as a function of increasing concentration of PPB and for equilibration time, $\tau_e \approx 0$, 1 day, and 7 days are shown in Fig. 1 a–c, respectively. The corresponding molar ratios, R_m-dependence of the thermotropic parameters, transition temperatures, and transition enthalpies, are given in Figs. 2a and 3a, respectively. The DSC heating scan of the gel phase of DPPE dispersion displays an endothermic transition the chain melting transition ($L_\beta \Leftrightarrow L_\alpha$) (Fig. 1a, $R_m = 0$). The chain melting transition temperature, T_m, and enthalpy, ΔH_m, associated with this transition are 63.7 °C and 40.3 kJ mol^{-1}, respectively. The observed thermotropic parameter values are in good agreement with those reported in the literature [16, 17].

From Fig. 1a (solid curves), it is observed that in PPB-doped DPPE dispersion, the CM transition is asymmetrically broadened toward lower temperature, and this asymmetry increases with the increasing PPB (for $R_m < 0.4$) concentration. This suggests the existence of micro domains composed of PPB-rich and PPB-poor regions. However, for $R_m > 0.3$, the transition width is reduced. The transition temperature, T_m, is found to decrease with increasing PPB concentration. Presence of PPB ($R_m \geq 0.1$) in DPPE dispersion results in the evolution of new transitions on the low temperature side (at approximately 35, 45, and 48 °C) of the CM transition (Fig. 1a). The transition temperature of the additional transitions did not show PPB-concentration dependence

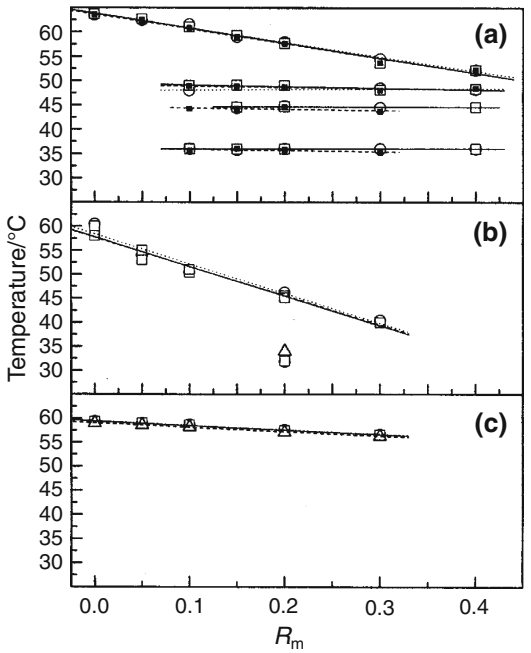

Fig. 2 R_m-dependence of transition temperatures, $T_{m/LC/HC}$ of **a** DPPE-PPB-buffer pH 7.4 **b** DPPE-ch-PPB-buffer pH 7.4, and **c** DPPE-PPB-buffer pH 9.3(ULV) systems for $\tau_e \approx 0$ (*circle*), $\tau_e \approx 1$ day (*square*), and $\tau_e \approx 7$ days (*triangle*). The size of the symbol has been chosen in conformity with the error bar. The *lines* connecting the data points have been drawn as a guide to the eye

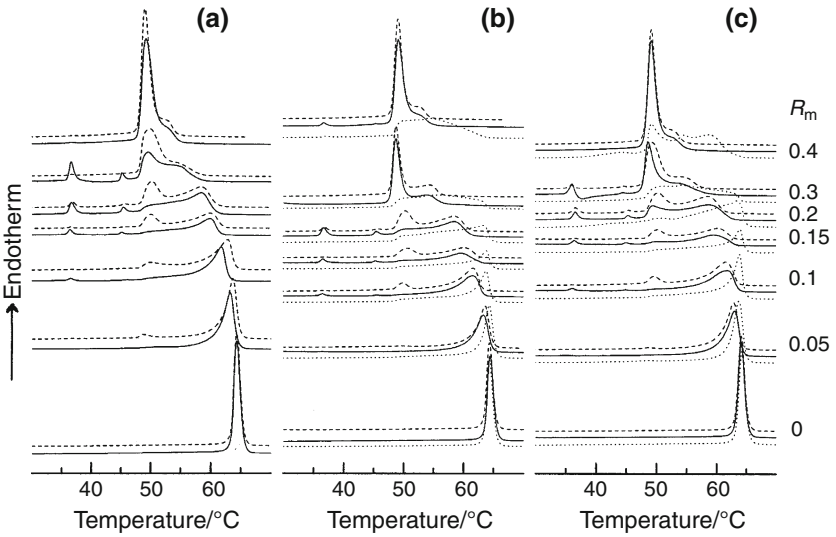

Fig. 1 The DSC heating profiles at 5 °C/min of DPPE-PPB-buffer pH 7.4 (MLV) containing different amount of PPB for **a** $\tau_e \approx 0$ **b** $\tau_e \approx 1$ day, and **c** $\tau_e \approx 7$ days. The molar ratio, R_m, of PPB to DPPE is indicated on the scans. 1st scan *dotted curve*, 2nd scan *solid curve*, heating scans obtained after cooling the samples to −20 °C *dash curve*

(Fig. 2a). However, the intensity of these addition transitions increases with increasing PPB concentration. The transition observed at 48 °C is probably due to the formation of crystalline L_{LC} phase (crystalline subgel phase with transition temperature, $T_{LC} < T_m$) [18]. The intensity of the L_{LC} phase formed is different for the same sample at different heating cycles with same scanning speed; the intensity is high at low scanning speed (2 °C/min). The intensity of L_{LC} phase increases in the case of heating scan recorded after the sample was cooled to −20 °C (Fig. 1a (dash curves)). For $R_m = 0.4$, wherein the intensity of the L_{LC} phase transition is high, the transition at 35 °C is not seen. From Fig. 3a, it is seen that the total transition enthalpy increases in the presence of PPB. This increase in enthalpy value is probably due to the formation of the crystalline L_{LC} phase.

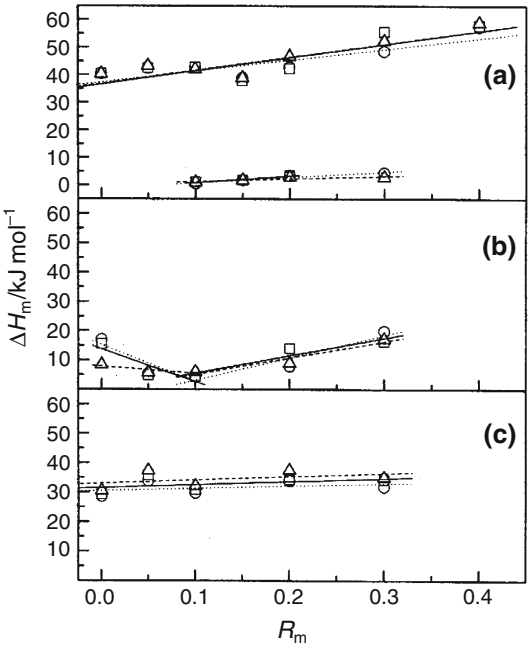

Fig. 3 R_m-dependence of total transition enthalpy ($\Delta H_{tot} = \Delta H_{m/LC/HC}$) **a** DPPE-PPB-buffer pH 7.4, **b** DPPE-ch-PPB-buffer pH 7.4, and **c** DPPE-PPB-buffer pH 9.3(ULV) systems for $\tau_e \approx 0$ (*circle*), $\tau_e \approx 1$ day (*square*), and $\tau_e \approx 7$ days (*triangle*). The size of the symbol has been chosen in conformity with the error bar. The *lines* connecting the data points have been drawn as a guide to the eye

The effect of addition of cholesterol(ch) to DPPE-PPB-pH 7.4 system is also investigated. The DSC heating profile of DPPE-ch dispersion both in the presence and absence of PPB for equilibration time, $\tau_e \approx 0$, 1 day and 7 days is shown in Fig. 4a–c. The corresponding molar ratio, R_m-dependence of the thermotropic parameters, the transition temperatures and the transition enthalpies, are given in Figs. 2b and 3b, respectively. Presence of cholesterol in DPPE dispersion broadens the CM transition and shifts the transition peak to lower value (60.2 °C). The transition enthalpy, ΔH_m, associated with this broad transition is approximately 17.0 kJ mol^{-1}. A small hump is also seen at about 31 °C. Cholesterol causes a fluidizing effect in DPPE vesicles. Similar effect is seen with dipalmitoyl phosphatidylcholine (DPPC)-ch system [19, 20]. On cooling the DPPE-ch dispersion to −20 °C, there is the evolution of new phases whose transition temperatures are approximately 17 °C and 21.7 °C and the total enthalpy associated with it is 3.4 kJ mol^{-1} (Fig. 4a ($R_m = 0$) dash curve).

Presence of PPB in DPPE-ch dispersion increases the CM transition width and decreases the transition temperature (Fig. 2b). For PPB concentration, $R_m \leq 0.1$ the transition enthalpy, ΔH_m, value decreases and with further increase in PPB concentration ($R_m \geq 0.1$) the transition enthalpy, ΔH_m, value increases (Fig. 3b). This increase in enthalpy value could be due to the formation of low temperature crystalline subgel phase. This behavior is similar to that seen with cholesterol-free DPPE-PPB system.

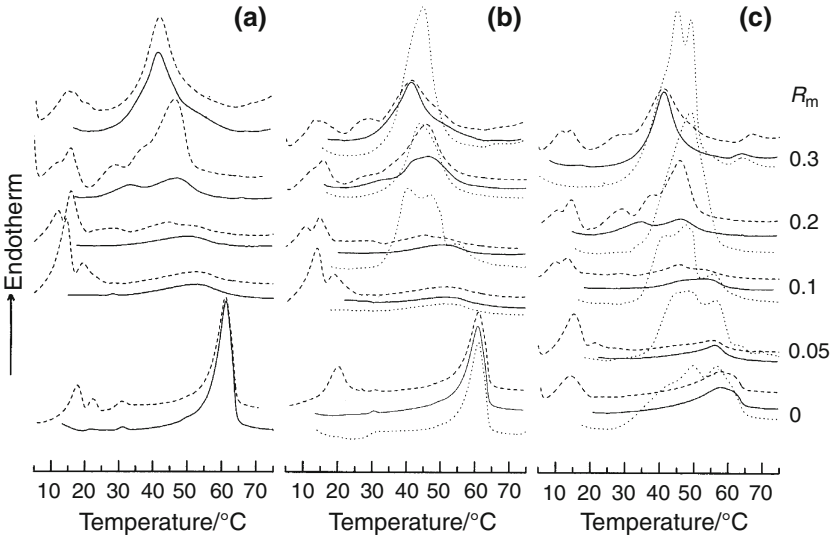

Fig. 4 The DSC heating scans at 5 °C/min of DPPE-ch-PPB-buffer pH 7.4(MLV) containing different amount of the PPB for **a** $\tau_e \approx 0$, **b** $\tau_e \approx 1$ day, and **c** $\tau_e \approx 7$ days. The molar ratio, R_m, of PPB to DPPE is indicated on the scans. 1st scan *dotted curve*, 2nd scan *solid curve*, heating scans obtained after cooling the samples to −20 °C *dash curve*

DPPE-ch-PPB dispersion when cooled to −20 °C also forms a new phase whose transition temperature is approximately 15 °C and seems to be similar to that seen in PPB-free DPPE-ch dispersion (Fig. 4a dash curve). The transition temperature of this new phase does not change significantly with increasing concentration of PPB. However, the transition enthalpy associated with this transition increases with increasing PPB concentration (Fig. 4a dash curves). The thermal values(T_m and ΔH_m) obtained from the DSC data indicate that for a given PPB concentration, the interaction of the PPB with DPPE is higher in the presence of the cholesterol.

$\tau_e \approx$ 1 and 7 days

The gel phase of DPPE ($R_m = 0$) and DPPE-ch ($R_m = 0$) systems when equilibrated for a day did not change the thermotropic parameters (Figs. 1b (dotted curves) and 4b (dotted curves) and Table 1) when compared to $\tau_e \approx 0$ values. However, when the gel phase of DPPE ($R_m = 0$) and DPPE-ch ($R_m = 0$) systems were equilibrated for 7 days, DPPE-ch system formed crystalline L_{LC} phase (Figs. 4c (dotted curves) and Table 1). However, the gel phase of DPPE-pH 7.4 system on equilibration did not form crystalline subgel phase. The gel phase of DPPE is known to be metastable and on equilibration gets converted to stable crystalline phase [21–24].

The first (dotted curve) and the second (solid curve) scans recorded with the equilibrated ($\tau_e = 1$ day) DPPE-PPB-buffer pH 7.4 samples indicate transformation of the gel phase to a crystalline subgel, L_{HC}, phase with transition temperature $T_{HC} > T_m$ (Fig. 1b and Table 1). On equilibration the subgel, L_{LC}, phase seen for $\tau_e \approx 0$ is transformed to subgel, L_{HC}, phase. Similar high temperature subgel phase formation is reported in dapsone-free and dapsone-doped DPPE-water systems [18]. The total transition enthalpy, ΔH_{tot} ($\Delta H_m + \Delta H_{HC}$), of the DPPE-PPB-buffer pH 7.4 system, increases on equilibration (Table 1). The subsequent DSC heating scans of DPPE-PPB-buffer pH 7.4 system are almost similar to that of $\tau_e \approx 0$ (Figs. 1a and b, 2a and 3a) (except for $R_m > 0.2$ where the intensity of subgel, L_{LC}, phase increases). Similar behavior was seen when the gel phase of DPPE-PPB-buffer pH 7.4 system was equilibrated for 7 days (Fig. 1c and Table 1). Equilibrating cholesterol-doped DPPE-PPB dispersion (for $R_m < 0.2$) at 25 °C for a day, does not result in the formation of any subgel phase and the DSC heating profiles are almost similar to those obtained for $\tau_e \approx 0$ (Fig. 4b first scan (dotted curves) and second scan (solid curves)). However, for $R_m > 0.1$, the first heating scan shows the presence of subgel phase (Fig. 4b (dotted curve) and Table 1). The subsequent DSC heating scans are almost similar to those of $\tau_e \approx 0$ (Figs. 2b, 3b and 4). However, when the cholesterol-doped DPPE-PPB dispersion was equilibrated for 7 days, there is the evolution of subgel phases for the entire PPB concentration range (Table 1). The subsequent DSC heating scans do not show any significant change (when compared with those of $\tau_e \approx 0$).

DSC—unilamellar vesicles

The DSC heating profiles, of the ULV of DPPE-PPB-buffer pH 9.3 system obtained at the scan rate of 5 °C/min, for $\tau_e \approx 0$ (solid curve), $\tau_e \approx 1$ day (dash curve) and $\tau_e \approx 7$ days (dotted curve) with increasing PPB concentrations are shown in Fig. 5. The R_m-dependence of the thermotropic parameters are given in Figs. 2c and 3c.

The DSC heating thermogram of DPPE dispersion in buffer pH 9.3, displays an endothermic chain-melting transition at a temperature 59.4 °C and the enthalpy, ΔH_m, associated with this transition is 28.5 kJ mol^{-1}. The T_m and ΔH_m values obtained are less than the corresponding ones for MLV probably due to reduced headgroup–headgroup interaction in the ULV form because of its high degree of curvature. The values of full width at half maximum, Δ_m, was increased and was nearly two folds that of MLV probably due to the presence of ULV with different size and/or few lamella(s).

From Figs. 2c, 3c and 5, it is seen that in PPB-doped DPPE dispersion, CM transition broadens and the transition temperature, T_m, is reduced. The transition enthalpy associated with this transition is increased. The presence of PPB seems to reduce the effective headgroup–headgroup interaction and increase the acyl chain order. This behavior is similar to that observed in MLV.

Thermotropic parameters obtained for samples equilibrated for 1 and 7 days at 25 °C, hardly shows any change, when compared with their $\tau_e \approx 0$ values (Figs. 2c and 3c). However, equilibration (Fig. 5) results in increased transition width for both PPB-free and PPB-doped DPPE dispersions. This could most probably be due to the formation of multibilayer vesicles of different sizes. The ULV is known to be unstable and fuse to form multilamellar vesicles [25].

^{1}H NMR—unilamellar vesicles

DPPE resonances

The ^{1}H NMR spectra of DPPE molecules in DPPE-buffer pH 9.3 and DPPE-PPB-buffer pH 9.3 ($R_m = 0.2$) for various temperatures in the vicinity of T_m are shown in Fig. 6a and b, respectively. Various proton resonances in the spectra can be identified with the assignments given in inset of Fig. 6. On comparing PPB-free and PPB-doped DPPE spectra, it is seen that in both cases, the chain

Table 1 R_m-dependence of the thermotropic parameters-the transition temperatures, (T_{LC}, T_{HC} and T_m) and the total transition enthalpy, ΔH_{total} ($\Delta H_{total} = \Delta H_{LC} + \Delta H_{HC} + \Delta H_m$) obtained after equilibrating the DPPE-PPB-buffer pH 7.4 and DPPE-ch-PPB-buffer pH 7.4 samples at 25 °C for $\tau_e \approx 1$ day and for $\tau_e \approx 7$ days

	1 day								7 days							
	DPPE-PPB-pH 7.4				DPPE-ch-PPB-pH 7.4				DPPE-PPB-pH 7.4				DPPE-ch-PPB-pH 7.4			
	1st heating		2nd heating		1st heating		2nd heating		1st heating		2nd heating		1st heating		2nd heating	
R_m	*T*/°C	ΔH (total)/ *kJ mol^{-1}	*T*/°C	ΔH(total)/ *kJ mol^{-1}	*T*/°C	ΔH(total)/ *kJ mol^{-1}	*T*/°C	ΔH(total)/ *kJ mol^{-1}	*T*/°C	ΔH(total)/ *kJ mol^{-1}	*T*/°C	ΔH(total)/ *kJ mol^{-1}	*T*/°C	ΔH(total)/ *kJ mol^{-1}	*T*/°C	ΔH(total)/ *kJ mol^{-1}
0	–		–		–	–	–		–		–		48.8_{LC}			
	64.5_m	40.7	63.7_m	40.1	60.2_m	18.5	60.0_m	15.5	64.2_m	42.6	63.7_m	40.5	56.0_m	35.3	58.0_m	8.5
0.05	–				–				48.0_{LC}				47.7_{LC}			
	63.7_m	52.1	62.7_m	42.5	50.3_m	4.5	53.0_m	4.8	63.2_m	44.0	62.5_m	43.3	56.2_m	37.4	55.0_m	5.8
0.1	–	–	36.0*	1.0	39.8_{LC}				–	–	35.6*	1.0	39.6_{LC}	41.9	51_m	6.1
	49.0_{LC}		49.0_{LC}		46.6_{LC}						48.9_{LC}		46.8_{LC}			
	63.0_{HC}	54.9	61.0_m	44.7	55.0_{HC}	40.0	50.4_m	4.4	63.2_m	55.4	60.8_m	42.0	55.7_{HC}			
0.15	–		36.0*	1.7							36.0*	1.7				
	–		44.6_{LC}								44.3_{LC}					
		49.0_{LC}	49.1_{LC}						49.2_{LC}		48.8_{LC}					
		63.0_{HC}	44.8	59.3_{HC}	37.8				63.0_{HC}	43.8	59.0_m	38.8				
0.2	–		36.0*	3.4		–					35.8*	2.9				
			44.7_{LC}								44.6_{LC}					
			49.0_{LC}						49.7_{LC}		48.7_{LC}					
	62.6_{HC}	69.9	57.7_m	42.2	$42.2_{LC/m}$	24.3	45.5_m	14.0	62.7_m	76.2	57.6_m	46.7	$48.0_{LC/m}$	51.9	45.1_m	9.0
0.3	–		–						–		35.3*	2.9				
	–		–						–		43.7_{LC}		$44.0_{HC/m}$	47.7	40.0_m	17.2
	48.6_{LC}		48.1_{LC}						–		48.0_{LC}		48.5_{HC}			
	54.7_m	62.9	53.7_m	55.5	$44.0_{HC/m}$	33.6	40.0_m	16.3	53.7_m	62.9	53.7_m	52.3	63.0_{HC}	1.1	63.0_{HC}	0.7
0.4	–	–	36.0*	1.0												
	44.8_{LC}		44.6_{LC}													
	–	–	48.3_{LC}						48.6_{LC}		48.4_{LC}					
	53.7_m	65.1	52.2_m	57.9					53.3_m	82.3	52.2_m	58.9				

LC low temperature crystalline phase, *HL* high temperature crystalline phase, *m* main transition

* New phase(s)

ΔH_{total}: $\Delta H_{LC} + \Delta H_{HL} + \Delta H_m$

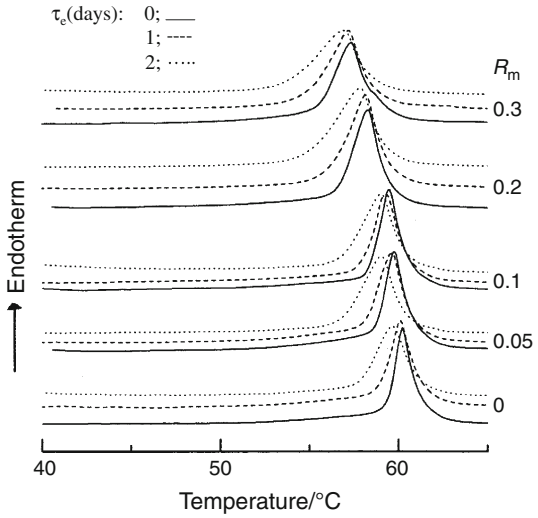

Fig. 5 DSC heating scans at 5 °C/min of ULV of DPPE-PPB-buffer pH 9.3 with increasing R_m as indicated on the curves (i) $\tau_e \approx 0$, *solid curve*; (ii) $\tau_e \approx 1$ day, *dash curve*; and (iii) $\tau_e \approx 7$ days, *dotted curve*

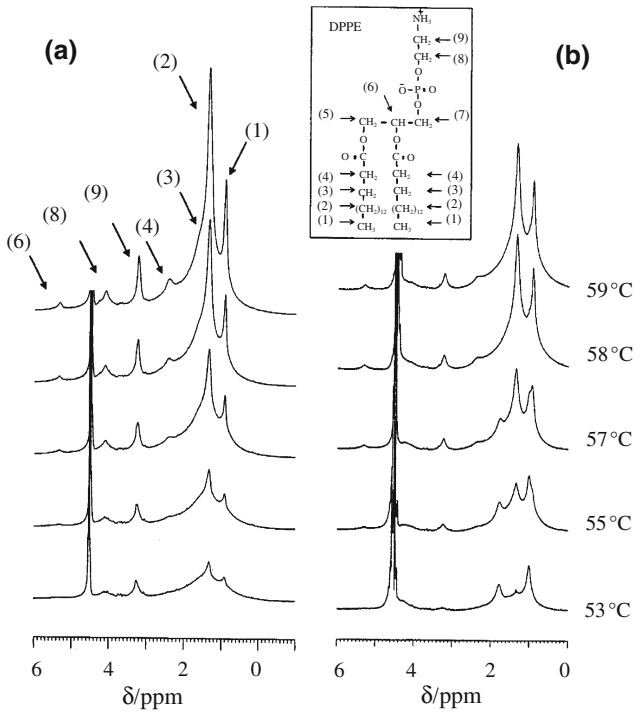

Fig. 6 ^{1}H NMR spectra of **a** DPPE ($R_m = 0$) and **b** DPPE-PPB ($R_m = 0.2$) dispersions in the vicinity of T_m. Assignments for the various groups of DPPE are given in the inset. [DPPE] = 25 mM

resonances (1) and (2) are broad and unresolved at temperature less than T_m. They start getting resolved and become sharper as the temperature approaches T_m. This sharp increase in chain proton resonance upon phase transition is indicative of increased mobility for the concerned proton due to increased chain disorder. Though the T_m of DPPE dispersion is affected by the presence of PPB, there is no significant change in the chemical shifts of the various lipidic resonances. However, the resonances of the various lipidic protons are considerably broadened in PPB-doped DPPE dispersion. The resonances labeled (8) and (9 (for $T < T_m$)) are hardly visible due to broadening. These results indicate that the mobility of lipidic protons is reduced in the presence of PPB. These results suggest that a PPB molecule interacts with the $-N^+H_3$ group, thereby reducing the electrostatic interaction between $-PO_4^-$ and N^+H_3 groups.

PPB resonances

The ^{1}H NMR spectra of the protons, labeled 11–17, from PPB in the aqueous medium, PPB-buffer pH 9.3 at various temperatures are shown in Fig. 7a. The concentration of PPB in the aqueous medium was same as that present in DPPE-PPB system with $R_m = 0.2$. The labeled PPB molecule is shown in the inset of the figure. The spectra of the aromatic protons of PPB obtained from DPPE-PPB dispersions at various temperatures around T_m are given in Fig. 7b. From Fig. 7a and b, it is seen that the PPB resonances are perturbed by the presence of DPPE. The perturbation is stronger for temperatures, $T > T_m$. The fine structure of the aromatic proton resonances of PPB almost disappears, as seen from the broadening of the resonances in the presence of DPPE. The broadening effect is more for temperature, $T > T_m$ (aromatic resonances hardly seen). The chemical shift (upfield shift) values of various aromatic protons of PPB decreases in the presence of lipid

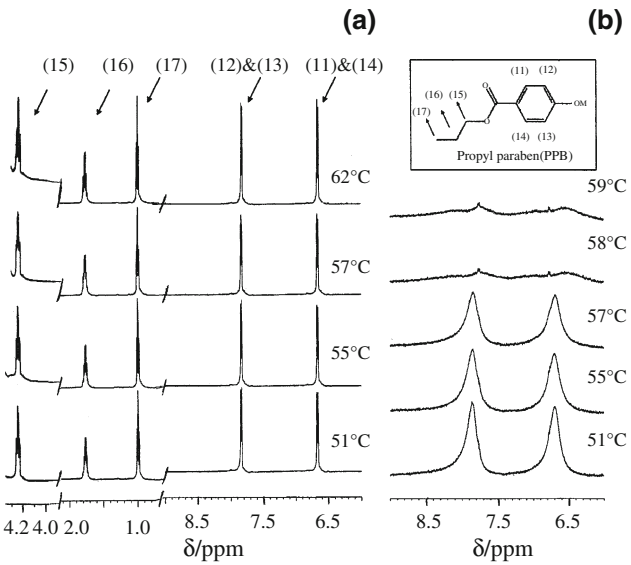

Fig. 7 ^{1}H NMR spectra of PPB in **a** PPB-buffer pH 9.3 and **b** DPPE-PPB-buffer pH 9.3 ($R_m = 0.2$) systems in the vicinity of T_m. Inset gives the assignment for PPB [DPPE] = 25 mM

environment. This could be due to the hydrogen bonding interaction between the polar groups of PPB and DPPE molecules. The proton resonances corresponding to the –OH group of PPB are not seen due to exchange processes. From Figs. 6b and 7a, it is seen that the proton resonances labeled 15, 16 and 17 of PPB, broaden significantly in DPPE environment and are hardly seen for temperature, $T > T_m$. These data suggest that the PPB molecules interact with the DPPE bilayer and the interaction is stronger at temperature, $T > T_m$. The ^{1}H NMR results suggest that the –OH group of PPB molecules are expected to be located near the lipid glycerol moiety and/or the polar headgroup, with its polar group interacting with (a) the vicinal water (b) the P=O (DPPE) group or (c) the C=O (lipid) group through hydrogen bonding.

^{31}P NMR—unilamellar vesicles

^{31}P NMR experiments were carried out with PPB-free and PPB-doped unilamellar vesicles of DPPE, to see whether the polar group of PPB interacts with the phosphate group of DPPE. The ^{31}P NMR spectra from the PPB-free and PPB-doped ULV of DPPE are presented in Fig. 8a and b, respectively. When the ^{31}P NMR line shapes obtained for pure DPPE and DPPE-PPB mixture are compared, it shows that the presence of PPB (a) significantly changes the ^{31}P NMR resonance pattern and (b) results in the chemical shift values becoming higher. These results suggest that presence of PPB molecules in DPPE dispersion reduces the electrostatic interaction between $-PO_4^-$ and $-N^+H_3$ groups.

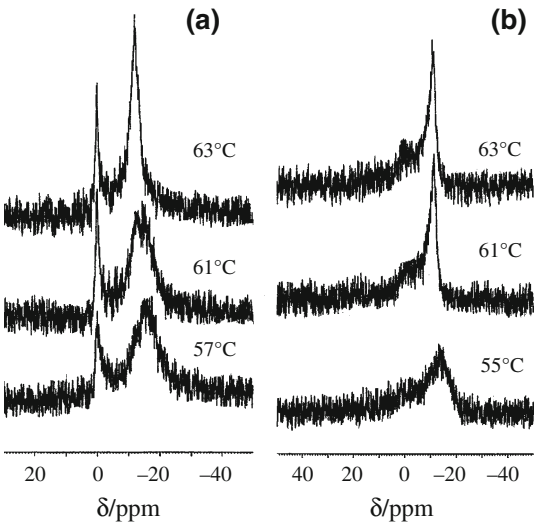

Fig. 8 Proton decoupled ^{31}P NMR spectra of **a** DPPE-buffer pH 9.3 and **b** DPPE-PPB-buffer pH 9.3 ($R_m = 0.2$) systems in the vicinity of T_m [DPPE] = 25 mM

Discussion

The DSC results of ULV and MLV indicate that the effect of the PPB on the DPPE bilayer is more or less the same in both forms. The decreased T_m value and ^{31}P NMR spectra of the PPB-doped DPPE dispersions suggest that the presence of PPB decreases the headgroup–headgroup interaction of the neighboring DPPE molecules. This is supported by the ^{1}H NMR results that the presence of DPPE leads to a reduction in the mobility of the aromatic protons of PPB. This effect is due to hydrogen bonding and or electrostatic interactions between the polar groups of PPB and DPPE molecules, which reduce the effective headgroup–headgroup interaction. Hence, the polar moiety of the PPB molecules gets intercalated between the polar groups of the phospholipids and its alkyl chain penetrating into the cooperative region. This is supported by the values of transition enthalpy and the chemical shift of the various DPPE proton resonances in the presence of PPB. From DSC results, it is found that the transition enthalpy increases with increasing PPB concentration. This increase in enthalpy is related to the formation of crystalline subgel phase. The gel L_β phase, of DPPE is known to be metastable and under appropriate conditions (low temperature equilibration), transforms to a stable crystalline subgel L_C phase [21, 22, 26–30]. This transformation leads to (a) a more ordered packing of the lipids within the bilayer and (b) the expulsion of most of the interlamellar water [29, 30]. The strong interactions between the PE headgroups (both intra- and inter-bilayer) are responsible for the metastability of the gel L_β phase in model membranes made up of diacyl PEs with saturated chains of length C_{10} to C_{16} [27, 31]. In cholesterol-doped DPPE vesicles, PPB brings about similar perturbation in the biophysical properties of the vesicles. However, for a given concentration of PPB, the influence of PPB on the biophysical properties is large in cholesterol-doped DPPE dispersion than that of cholesterol-free DPPE dispersion. Hence, the above results suggest that PPB perturbs the biophysical properties of DPPE vesicles. This could be of pharmacologic importance.

Study carried out with PPB-doped DPPC system showed that PPB interacts with DPPC membrane by affecting both its thermotropic behavior and molecular mobility [12]. In both DPPE and DPPC dispersions, the presence of PPB increases the fluidity of the polar headgroup by decreasing the headgroup–headgroup interaction. In DPPC dispersion, PPB reduces the acyl chain order. However, in DPPE dispersion, the presence of PPB increases the acyl chain order, most probably due to the formation of crystalline subgel phase. These differences may be related to the fact that PE–PE interaction is stronger than PC–PC interaction.

Equilibration ($\tau_e \approx$ 1 day and 7 days) of MLV, of PPB-doped DPPE-buffer pH 7.4 and PPB-free and PPB-doped

DPPE-ch-buffer pH 7.4 at 25 °C, resulted in the formation of a crystalline subgel phase(s)(L_{LC} and L_{HC}). The gel phase of DPPE-buffer pH 7.4 does not form subgel phase on equilibration. The gel phase of DPPE-buffer pH 7.4 and DPPE-ch-buffer pH 7.4 dispersions, in presence of appropriate PPB concentration, transforms to a stable crystalline subgel phase with shorter equilibration time. These results suggest that PPB acts as a catalyst for gel phase to subgel phase(s) transformation. The PPB also enhances the intensity of the subgel phases.

The subgel L_{HC} phase → L_{β} phase transition is indicative of the simultaneous hydration and acyl chain melting of a poorly hydrated crystalline sample, which gives rise to big change in total transition enthalpy [23]. The transition enthalpy of the metastable gel L_{β} phase → L_{α} phase corresponds only to the melting of the acyl chains. Similar to subgel, L_{HC} phase, in the L_{LC} phase also the acyl chain order is increased but with less inter-bilayer water sequestering out. The formation of somewhat similar low temperature subgel phase in aqueous dispersions of dimyristoyl phosphatidylethanolamine (DMPE) has been reported earlier [32, 33].

Schematic model for the likely location of PPB molecules in DPPE bilayer is shown in Fig. 9. PPB with pK_a value of 8.47 will have negatively charged –OH group at pH 9.3. Hence, there can be electrostatic attractive interaction between the $–O^-$ group of PPB molecules and the $–N^+H_3$ group of DPPE. This results in reduced interaction between the $–PO_4^-$ and N^+H_3 groups of the DPPE molecules. The ^{31}P NMR experiment with DPPE-PPB-buffer pH 9.3 has shown that the phosphorous resonances are perturbed by the presence of PPB. Thus, the interaction between PPB and DPPE molecules are as represented in (B) (Fig. 9). However, when the DPPE dispersion is prepared in buffer pH 7.4, the PPB molecules will be neutrally charged. Therefore, the –OH group of PPB can form hydrogen bonding with the (a) vicinal water or (b) the –P=O (DPPE) group or (c) the –C=O (DPPE) group as represented by (A) (C), and (D) in Fig. 9. The presence of PPB molecule between DPPE molecules in the bilayer would increase the separation between headgroups, thereby weakening the PE–PE interactions, thereby enhancing the fluidity of DPPE headgroups. The formation of the more ordered crystalline $L_{LC/HC}$ phases can be explained by the strong intra- and inter-bilayer hydrogen bonding interaction between the neighboring PE headgroups. This facilitates the subgel $L_{LC/HC}$ phases formation by sequestering out the inter-bilayer water [31].

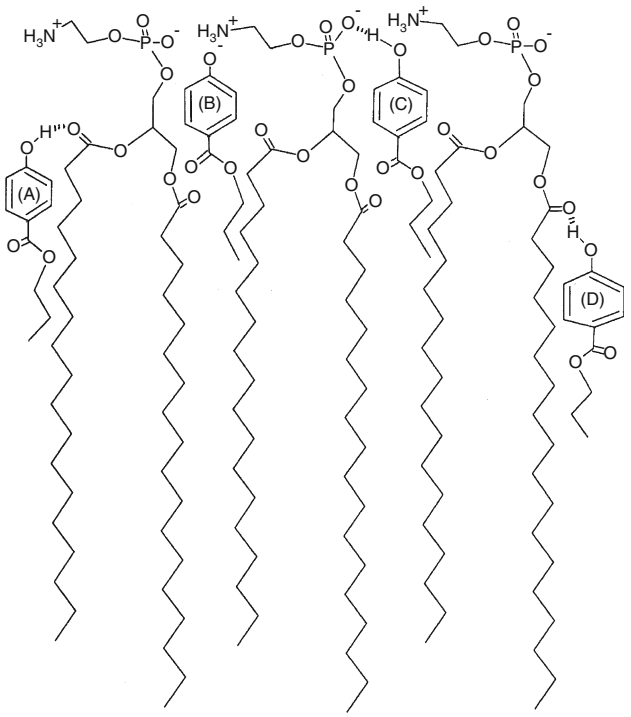

Fig. 9 Schematic model representing the location of PPB molecule in DPPE bilayer

Conclusions

The results clearly indicate that PPB strongly interacts with DPPE bilayer and gets intercalated between the polar groups of the phospholipids. PPB increases the headgroup fluidity by reducing PE–PE headgroup interaction. The modification of the fluidity of the model membrane may be an important factor in determining the functions of biomembranes and those of the molecules embedded in them. Presence of PPB seems to favor the formation of subgel L_{LC} phase. Equilibration studies suggest that PPB molecules are very strongly bound and remain intercalated between the polar headgroups for prolonged time. This finding could be of physiologic importance as parabens have been detected in human breast tumor tissue [9].

References

1. Soni MG, Burdock GA, Taylor SL, Greenberg NA. Safety assessment of propyl paraben: a review of the published literature. Food Chem Toxicol. 2001;39:513–32.
2. Elder RL. Final report on the safety assessment of methylparaben, ethylparaben, propylparaben, and butylparaben. J Am Coll Toxicol. 1984;3:147–209.
3. Perlovich GL, Rodionov SV, Bauer-Brandl A. Thermodynamics of solubility, sublimation and solvation processes of parabens. Eur J Pharm Sci. 2005;24:25–33.
4. Eklund T. Inhibition of growth and uptake processes in bacteria by some chemical food preservatives. J Appl Bacteriol. 1980;48:423–32.

5. Eklund T. The effect of sorbic acid and esters of p-hydroxybenzoic acid on the protonmotive force in Escherichia coli membrane vesicles. J Gen Microbiol. 1985;131:73–6.
6. Freese E, Levin BC. Action mechanisms of preservatives and antiseptics. Dev Incl Microbiol. 1978;19:207–27.
7. Freese E, Shen CW, Galliers E. Function of lipophilic acids as antimicrobial food additives. Nature. 1973;241:321–4.
8. Harvey PW, Everett DJ. Significance of the detection of esters of p-hydroxybenzoic acid (parabens) in human breast tumours. J Appl Toxicol. 2004;24:1–4.
9. Darbre PD. Environmental oestrogens, cosmetics and breast cancer. Best Practice Res Clin Endocrinol Metabol. 2006;20: 121–43.
10. Gennis RB. Biomembranes: molecular structure and function. New York: Springer; 1989.
11. Panicker L. Effect of propyl paraben on the dipalmitoyl phosphatidic acid vesicles. J Colloid Interface Sci. 2007;311:407–16.
12. Panicker L. Interaction of propyl paraben with dipalmitoyl phosphatidylcholine bilayer: a differential scanning calorimetry and nuclear magnetic resonance study. Colloids Surf B Biointerfaces. 2008;61:145–52.
13. Panicker L, Narasimhan SL, Mishra KP. Reduced fluidity of dipalmitoyl phosphatidic acid membranes by salicylic acid. Thermochim Acta. 2005;432:41–6.
14. Panicker L, Mishra KP. Salicylic acid-induced effects in the mixed-lipid (dipalmitoyl phosphatidylcholine–dipalmitoyl phosphatidylethanolamine) model membrane. J Colloid Interface Sci. 2005;290:250–8.
15. Panicker L, Mishra KP. Nuclear magnetic resonance and thermal studies on the interaction between salicylic acid and model membranes. Biophys Chem. 2006;120:15–23.
16. Koynova R, Caffrey M. Phases and phase transitions of the hydrated phosphatidylethanolamines. Chem Phys Lipids. 1994;69:1–34.
17. Stümpel J, Harlos K, Eibl H. Charge-induced pretransition in phosphatidylethanolamine multilayers. The occurrence of ripple structures. Biochim Biophys Acta. 1980;599:464–72.
18. Panicker L. Influence of the leprosy drug, dapsone on the model membrane dipalmitoyl phosphatidylethanolamine. Thermochim Acta. 2006;447:123–30.
19. Ladbrooke BD, Williams RM, Chapman D. Studies on lecithin-cholesterol-water interactions by differential scanning calorimetry and X-ray diffraction. Biochim Biophys Acta. 1968;29 (150):333–40.
20. Oldfield E, Chapman D. Dynamics of lipids in membranes: heterogeneity and the role of cholesterol. FEBS Lett. 1972;23:285–97.
21. Tenchov BG, Lis LJ, Quinn PJ. Structural rearrangements during crystal–liquid–crystal and gel–liquid–crystal phase transitions in aqueous dispersions of dipalmitoylphosphatidylethanolamine. A time-resolved X-ray diffraction study. Biochim Biophys Acta. 1988;942:305–14.
22. Vaughan DJ, Keough KM. Changes in phase transition of phosphatidylethanolamine—and phosphatidylcholine—water dispersions induced by small modifications in the head group and backbone region. FEBS Lett. 1974;47:158–61.
23. Mantsch HH, Hsi SC, Butler KW, Cameron DG. Studies on the thermotropic behavior of aqueous phosphatidylethanolamines. Biochim Biophys Acta. 1983;728:325–30.
24. Horniak L, Kutejova E, Balgavy P. Effect of phase transitions in hydrated 1,2-dipalmitoylphosphatidylethanolamine bilayers on the spin probe order parameter. FEBS Lett. 1987;224:283–6.
25. Lin BZ, Yin CC, Hauser H. The effect of positive and negative pH-gradients on the stability of small unilamellar vesicles of negatively charged phospholipids. Biochim Biophys Acta. 1993;1147:237–44.
26. Tenchov B, Koynova R, Rapp G. New ordered metastable phases between the gel and subgel phases in hydrated phospholipids. Biophys J. 2001;80:1873–90.
27. Lewis RNAH, McElhaney RN. Calorimetric and spectroscopic studies of the polymorphic phase behavior of a homologous series of n-saturated 1, 2-diacyl phosphatidylethanolamine. Biophys J. 1993;64:1081–96.
28. Kodama M, Inoue H, Tsuchida Y. The behavior of water molecules associated with structural changes in phosphatidylethanolamine assembly as studied by DSC. Thermochim Acta. 1995;266:373–84.
29. Mulukutla S, Shipley GG. Structure and thermotropic properties of phosphatidylethanolamine and its N-methyl derivatives. Biochemistry. 1984;23:2514–9.
30. Chang H, Epand RM. The existence of a highly ordered phase in fully hydrated dilauroylphosphatidylethanolamine. Biochim Biophys Acta. 1983;728:319–24.
31. Seddon JM, Harlos K, Marsh D. Metastability and polymorphism in the gel and fluid bilayer phases of dilauroylphosphatidylethanolamine. Two crystalline forms in excess water. J Biol Chem. 1983;258:3850–4.
32. Wilkinson DA, Nagle JF. Metastability in the phase behavior of dimyristoylphosphatidylethanolamine bilayers. Biochemistry. 1984;23:1538–41.
33. Hentschel MP, Braun S, Dietrich R, Trahms L. NMR and X-Ray investigation of the phase behavior of phosphatidylethanolamines. Mol Cryst Liq Cryst. 1985;124:205–17.